Temperature evolution in the deformation of bulk metallic glasses

by

Stephanie K. Slaughter

A thesis submitted to The Johns Hopkins University in conformity with the requirements for the degree of Master of Science in Engineering.

Baltimore, Maryland

May, 2014

Abstract

To determine the extent of heating in the deformation of bulk metallic glasses, a fusible tin coating method was used to detect shear band heating in amorphous $Zr_{57}Ti_5Cu_{20}Ni_8Al_{10}$ loaded under quasi-static uniaxial compression. A negative tone photolithography process was used to pattern tin lines 15μm wide with 5μm spacing on the metallic glass specimens. Quasi-static compression tests at a constant strain rate were performed using a high-stiffness, low-bending testing machine. Some samples were allowed to fracture while others were arrested before fracture. High-rate load data was acquired with a piezoelectric load cell and allowed for a precise determination of the time scale associated with the shearing events as well as final fracture. For samples where loading was halted prior to fracture there was no observed evidence of melted tin despite large shear offsets. For the samples loaded to fracture, there was evidence of melted tin near the fracture surface. These observations were attributed to the characteristic time scale of these events, measured from the load data. Temperature rise calculations were performed for both cases and it was found that the shear banding events with a time $t \sim$6 ms resulted in a $\Delta T < 1$ K while the

ABSTRACT

fracture event with a time $t \sim 30\mu$s resulted in $\Delta T \approx 2900$K. These calculations and results are consistent with other similar studies leading to the conclusion that there is no significant temperature rise in the normal deformation of bulk metallic glasses.

Acknowledgments

I would like to thank Dr. Todd Hufnagel for giving me the opprotunity to work on this project and inspiring an interest in a material I was before completely unfamiliar with. With his guidance and help from Erin Deda and Felicitee Kertis, former members of the Hufnagel Group, I was grateful to learn a variety of new laboratory techniques while also honing my skills as a researcher. Additionally, I am particularly thankful for the opprotunity to work with Dr. Wendelin Wright and Dr. Xiaojun Gu at Bucknell University, for without the use of their testing system our results would be less convincing. Finally, I would like to thank the entire Hufnagel Group for support throughout this research process.

Contents

CONTENTS

List of Tables

List of Figures

Chapter 1

Introduction

Metallic glasses and bulk metallic glasses (BMGs), first fabricated in the 1960s and 1990s respectively, demonstrate exceptionally unique mechanical properties. Between a tensile strength twice that of steel, fracture toughness higher than ceramics and comparable to alloys, considerable hardness, high fatigue strength, excellent corrosion resistance, and the molding abilities of soft materials, metallic glasses have remarkable potential. Prospective applications include but are not limited to magnetics, optics, sporting goods, electrodes, and structural materials [6]. The majority of these applications, however, are hindered by the underlying deformation mechanisms in metallic glasses which cause brittleness under large loads and ultimately catastrophic failure. As a result, interest has developed around elucidating the fundamental mechanisms that dictate the mechanical properties of metallic glasses, especially those encompassing deformation, on the atomic scale.

The majority of metallic glass research has since focused on expanding scientific understanding of the dependence of metallic glass properties on its amorphous structure. While models and experiments have demonstrated to an extent how metallic glasses deform, various aspects of this process are still unknown and debated [1, 6, 7]. With respect to deformation, there is a general consensus regarding the general motion of atomic displacements due to strain. These displacements can cause localized softening which leads to the propagation of atomic displacements along a single plane referred to as shear banding (sec 1.2). However, due to the rapid formation and localization of shear banding, there is still inadequate information about the exact nature of the deformation process and related properties.

One debated facet of metallic glass deformation that is still ineffectually explained is the presence of a temperature increase associated with shear bands. The work done for this thesis focuses on discussing the pertinent previous experimental attempts concerning this phenomenon (sec 1.4), describing our improved experimental methods to probe heating (sec 2), and, finally, outlining the results from our experiments and the implications on current metallic glass knowledge and research (sec 3).

1.1 Formation of Metallic Glasses

Metallic glasses are formed from the stabilization of a liquid alloy, undercooled below its melting temperature and before its glass transition is reached, thus "freezing"

atoms in an amorphous state. Since the first experiments of rapid-quenching on Au-Si alloys [8], numerous systems have been identified as having glass forming abilities. The typical parameters under which metallic glasses form have been identified as an interaction between multiple components, differing atomic sizes, and a negative enthalpy of mixing [6]. Experiments varying the composisition of the system, increasing cooling rates, and increasing the amount of undercooling have lead to improvements in the critical casting thickness, with thicknesses increasing from millimeters to centimeters, allowing for the formation of bulk metallic glasses (BMGs) [6, 7]. There are two typical methods for the production of BMGs: 1) solidification and 2) consolidation. Solidification simply consists of rapidly cooling the liquid alloy by suction casting into a copper mold acting as a heat sink. Consolidation refers to hot pressing or warm extrusion of amorphous powders in the supercooled region and can also be effectively be used. Regardless of teh formation technique that is employed, the resulting material will be a unique combination of metallic bonding and amorphous structure. As a result of this hybrid structure, the properties of metallic glasses exhibit characteristics between those of traditional crystalline metals and traditional oxide glasses.

1.2 Deformation Mechanisms

In contrast to metallic glasses, crystalline deformation has been thoroughly studied and can be categorized into elastic and plastic deformation mechanisms. In elastic deformation, intermolecular forces are sufficient enough to resist an applied force, any strain is reversed with an unloading of force and no structural change is observed. Conversely, plastic deformation is a low-energy process involving the breaking of atomic bonds by the movement of dislocations and is irreversible upon the unloading of force. Dislocation movement allows for crystalline planes to slip past one another, agglomerating into macroscopic shear bands and consequently producing irreversible structural deformation. It is also noted that although dislocations allow for slip, they can also cumulate and inhibit further slip; this process is referred to as strain hardening a material. These mechanisms rely on an ordered, crystalline atomic structure and are therefore not applicable to the amorphous structure in metallic glasses, Nonetheless, understanding these mechanisms is critical to understanding how thet properties of metallic glassese are different.

Without the presence of dislocations (defined as a defect in a crystalline order and thus not applicable), the breaking of atomic bonds in metallic glasses is a high-energy process. The exact process of atomic movement has yet to be fully elucidated but is generally thought of as a local rearrangement of atoms to a location of higher free volume to accommodate strain [9]. Shown in fig 1.1 are two proposed mechanisms defined by (a) a shear transformation zone (STZ) and (b) a more localized atomic

jump model. The STZ model suggests a region of atoms moves from one low energy

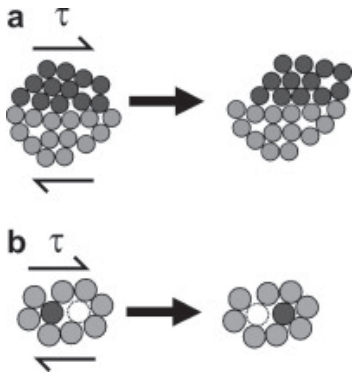

Figure 1.1: Proposed deformation mechanisms of (a) STZ and (b) local atomic jump. Reprinted from Schuh et. al [1].

configuration to another due to the applied force. The STZ area is considered to be on the order of tens to hundreds of atoms based on sophisticated computer simulations of metallic glasses. STZs are very complicated mechanisms, not considered a defect as in crystals but are a difference between two states, susceptible to orientation, short-range local order, local free volume, and ergodics of energy states [**?**]. The jump model is much more localized in which atoms jump into vacancies and shows a more diffusive characteristic. Primarily distinct in macroscopic effects, both of these processes are subjective to the same factors and share certain characteristics and consequences, such as being thermally activated [1], such as rearranging of free volume. The importance of these two modes is noted as they provide the foundation on which elastic and plastic deformation is understood in metallic glasses. The main consideration in this thesis is given to the irreversible plastic deformation, as it is this

which inhibits the usage of metallic glasses.

1.2.1 Plastic deformation and shear bands

Plastic deformation in metallic glasses can be described as STZs operating and rearranging free volume, resulting in an accumulation of strains. These events can occur homogeneously or inhomogeneously depending on factors such as temperature and strain rate. Main considerations here are given to inhomogeneous flow as this process generates localized shear banding and ultimately induces failure. Inhomogeneous flow relates to flow instability and occurs at high strain rates and low temperatures. In this mode, the local STZ rearrangements induces local softening which promotes additional STZ rearrangements and free volume can accumulate. This process is known as shear banding, the line of deformation is the shear band (fig 1.2), and the accumulation of free volume is the shear offset.

The shear banding process can be observed on stress-time or stress-strain curves obtained from either compression or tensile testing. As the applied load increases, shear bands are produced and propagate to accommodate the strain. As the shear offset occurs the measured load suddenly drops due to the changing material dimensions. Several load drops or serrations typically occur in the elastic and plastic region of the stress-strain curve before fracture, the number of drops depending on the ductility of the sample.

Shear bands can operate very rapidly, produce shear offsets up to millimeters,

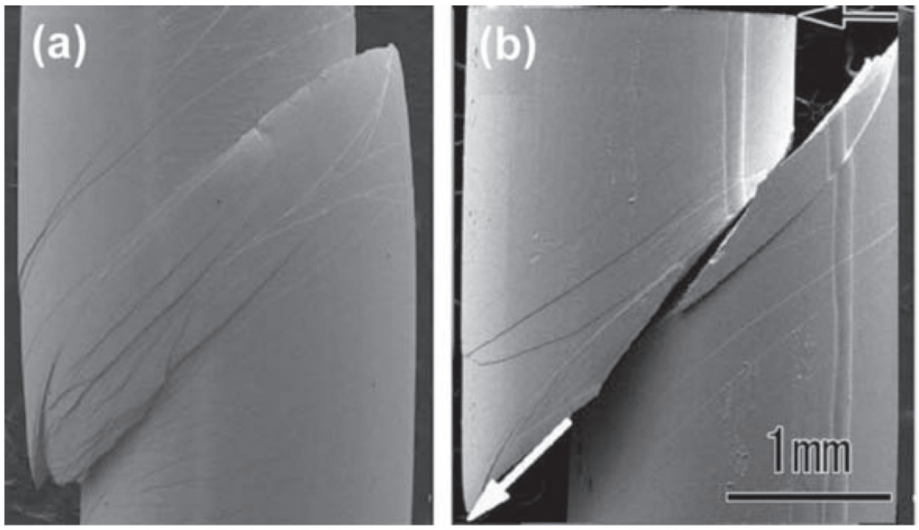

Figure 1.2: Scanning microsope images of (a) shear bands and shear offset and (b) the resulting failure. Reprinted from Louzguine-Luzgin et. al [2].

induce additional shear banding, and culminate in large plastic strain and macroscopic failure. As the prelude to failure, shear banding is one of the most important and debated mechanisms in metallic glass research. While certain aspects of shear band behavior have been established, others such as the rate of shear band propagation and the extent of heat released during the process are still debated [1, 10–12].

1.3 Fracture

Depending on the composition of a metallic glass, fracture can be characterized somewhere between semi-ductile to very brittle [6]. Again, due to lack of intrinsic strengthening mechanisms, cracks and shear bands can move and combine, unin-

hibited until the material fails. Although the fracture mechanism is ultimately the limiting reason preventing these materials from being used structurally, there has been little research on the subject. Experimental measurements of fracture toughness and fatigue limits have been performed extensively on various metallic glass systems, however the underlying atomic mechanisms occur so swiftly they have been difficult to characterize. The nist noteworthy observation regarding the fracture mechanism is the vein-like morphology found on metallic glass fracture surfaces (fig 1.3). While this pattern is generally associated with ductile fracture it is in fact a result of the apparent high temperatures at least exceeding the glass transition temperature - metallic glasses reach upon fracture.

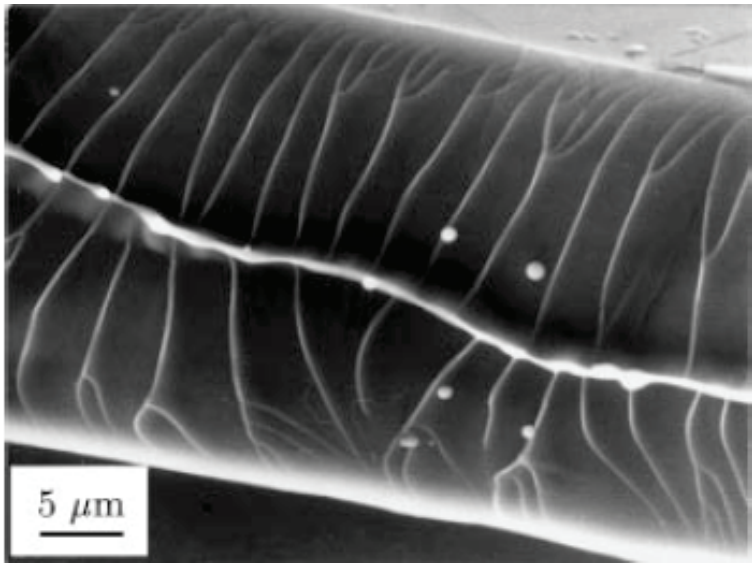

Figure 1.3: Scanning microsope images molten vein-like patterns on metallic glass fracture surface. Reprinted from Bengus et. al [3].

This is a critical feature inspiring various assumptions in metallic glass research which will be discussed in the next section.

1.4 Heat Evolution

It was first theorized that high temperature rises could be achieved during fracture due to the molten patterns on metallic glass fracture surfaces [7] and hot particles ejected during the fracture of Zr-based glasses [13]. However, an accurate measurement of this temperature rise and an answer to whether the heat evolution is associated with the initial shear banding deformation, or if it occurs during fracture, has proven difficult to ascertain due to the spatial and temporal resolutions neccessar for these experiments. The key spatial dimension needed to precisely evaluate temperature rises is directly related to the thickness of a shear band. With a very thin shear band, as compared to the size of the specimen, temperature increases would be impeded by heat conduction away from the band. While scanning electron microscopy measurements indicate band thicknesses of 10-20nm in smaller specimens [**?**, 14], it is uncertain whether the same dimensional ratios hold for bulk specimens. The key temporal resolution is the time scale of a shear banding event. Recent measurements using high-speed cinematography and high-acquisition data of load drops during serrated flow show the characteristic time for shear band operation is on the order of milliseconds [11, 15].

Although capturing the very localized and fast behavior of shear bands is very difficult, experimental resolutions have steadily improved. To be specific, direct infrared thermography experiments [12, 16] improved resolutions to $\sim$ 10 μm and 2.5 ms and found small temperature increases ($<$ 20K). However, assumptions about the true shear band thickness and shear band operation times were still required and conversation of direct temperature measurements inferred increases upwards of 1273K.

One method to circumvent these problems was produced by Lewandowski and Greer [4] who employed an indirect fusible coating method with spatial and temporal resolutions ($\sim$100 nm and $\sim$30 ps, respectively) sufficient, in principle, to estimate the heat evolved during shear band operation. By coating a metallic glass bend specimen with a thin layer of tin and observing melting near shear bands on the surface after fracture (fig 1.4), they demonstrated temperature rises of at least 200 K. The estimated temperature rise in this technique depends sensitively on the assumption made about the time scale of the shear banding event. Taking the transverse speed of sound as an upper limit on the shear velocity, Lewandowski and Greer calculated a theoretical maximum temperature rise of several thousand degrees. Later, Georgarakis and coworkers [17] explored the effect of the time scale assumption and calculated a range of possible maximum temperatures from 3400 K-8600 K for fast shear times ($\sim$10 ns) to an insignificant rise for slow shear times (100 ms). They therefore concluded that, because melted tin is observed near the shear bands, that the shear time must be

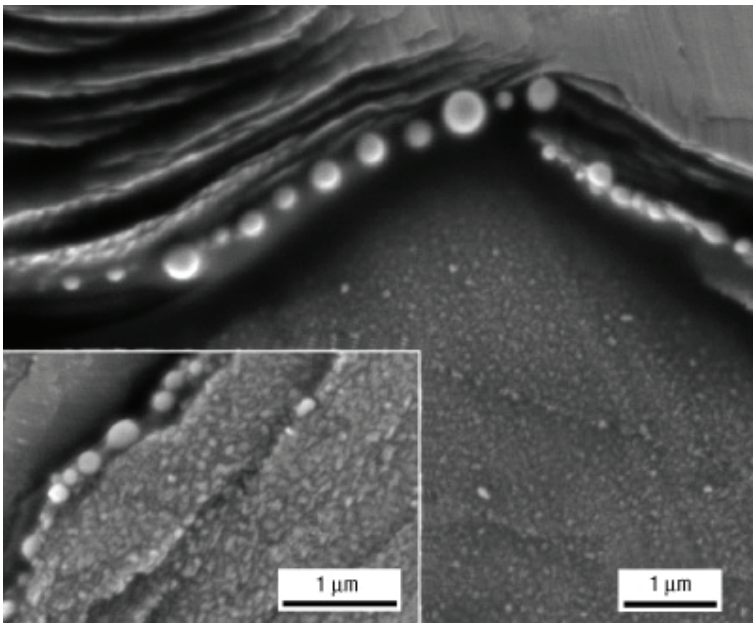

Figure 1.4: Scanning microsope image of the "fusible coating" melted at slip steps after bend testing. Reprinted from Lewandowski et. al [4].

short. Miracle and coworkers [18] revisited initial heat calculations from the fusible coating method and determined a critical slip offset of $\sim 10\mu$m (depending on sample size) would result in significant heating to be consistent with the observed melting of the tin coating.

On the other hand, Ketov and Louzguine-Luzgin [5] noted that in the original Lewandowski and Greer experiments the samples where melted tin was observed had been subjected to fracture (although the shear bands examined were well away from the fracture surface). As the strain energy released during the fracture event could dissipate much more heat to the initial shear bands, the conclusion that the shear bands were solely responsible for the melted tin may have been faulty. Using the

same fusible coating method they reported no melting of low-melting point metals near shear bands of specimens that did not fracture.

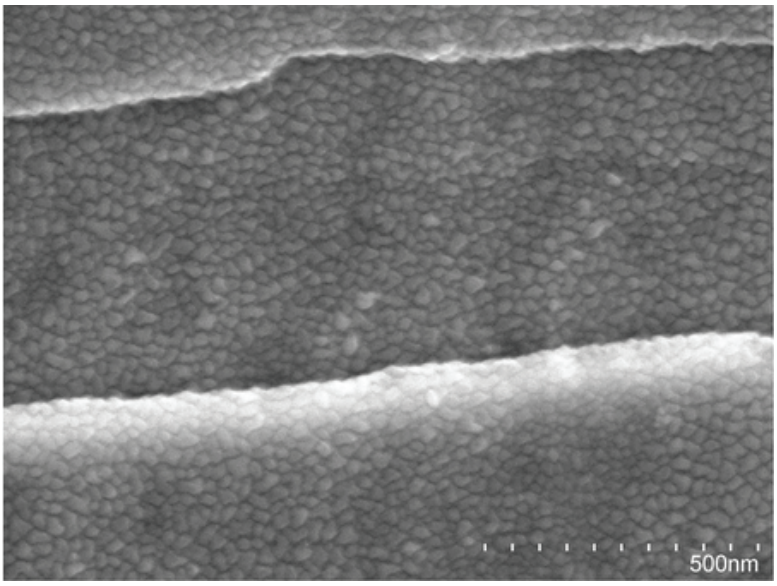

Figure 1.5: Scanning microsope images of unmelted fusible coating at slip steps after compression testing. Reprinted from Ketov et. al [5].

The discrepancy between all these different temperature rise analyses indicate how important it is to experimentally measure and ascertain within an order of magnitude the input parameters. Specifically the relation between shear velocity, heat diffusion, and maximum temperature rise requires more precise characterization. This work investigates this issue in greater detail, by performing additional fusible coating experiments on metallic glass compression specimens with two new features intended to help answer questions left open by prior work.

Chapter 2

Methods and Materials

Rectangular prism bulk metallic glass specimens of $Zr_{57}Ti_5Cu_{20}Ni_8Al_{10}$ (compositions in atomic percent) with dimensions 10.0 mm $\times$ 5.0 mm $\times$ 4.5 mm were fabricated by melting the constituents in an arc melter and subsequent suction casting into a copper mold. The amorphous atomic structure was verified by performing an X-ray Diffraction scan (PANalyticals X-PERT XRD using a PIXcel3D detector scanning from $2\theta = 5^\circ$ to 120° with Cu Kα radiation λ=1.5422$\mathring{A}$) on a slice from each end of the casted bar. The bar was cut into specimens of the specified dimensions. The specimens were polished on two adjacent sides to a mirror finish using 400, 600, 800, and 1200 SiC grit paper followed by a 1μm and 0.3μm alumina suspension. A pattern of vertical tin lines 15μm thick with 5μm spacing was placed on the two polished sides using a negative tone photolithography process (photolithography chemicals obtained from Futurrex, Inc.). The photolithography process was carried out as follows.

First the sample was plasma oxidized for 1 minute followed by spin coating negative photoresist NR9-1000PY on one side for 40 seconds at 3000 rpm. The pre-bake was done on a 150°C hotplate for 4 minutes. The sample was then exposed to UV light ($\lambda = 365$ nm) for 1minute through a mask followed by the post exposure bake on a 100°C hotplate for 210 seconds. Three milliliters of resist developer RD6 were dropped on the sample using a pipette and allowed to sit for 3 seconds before being immersed in DI water for 1 minute. A 50 nm layer of tin was deposited using a sputtering chamber at 30 Watts for 150 seconds (Sn target 99.999% purity; base pressure 10–7 Pa). The sample was then submerged in resist remover RR4 at 100∘C for 1 minute, leaving only the pattern of tin lines. This process was repeated for the second polished side, using a strip of aluminum foil to cover the already patterned side. Thickness of the tin lines was verified using profilometer measurements. Figure 2.1 shows images of the deposited tin lines.

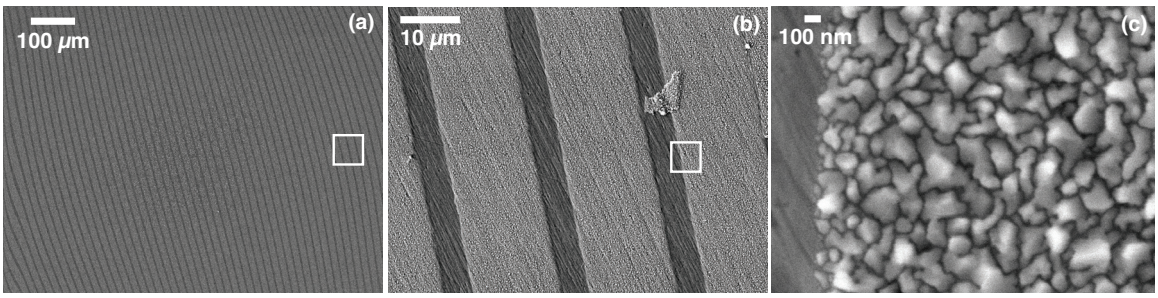

Figure 2.1: Scanning electron micrographs of deposited tin lines on a metallic glass specimen, prior to compression testing. Outlined in (a) and (b) are images (b) and (c) respectively.

CHAPTER 2. METHODS AND MATERIALS

Compression tests were performed under displacement control in quasi-static compression at displacement rate of $10^{-4}s^{-1}$ using a high stiffness, low-bending testing machine described in detail by Wright et. al [11,19]. Load data were acquired using a 250 kN Instron load cell and a Kistler piezoelectric load cell at 100 kHz. Displacement of the specimen was acquired using an Epsilon Tech extensometer. For six specimens the test was arrested after observing ∼5-10 load drops. Bending was minimized by use of a subpress, and high stiffness of the machine ensured minimal energy transfer from the system to the samples. Three samples were brought to fracture and six arrested before fracture and after shear band propagation, where shear band formation was indicated by a live view serrations in the load-time data. High-resolution field emission scanning electron microscopy (JOEL model JSM-6700L) was used to examine the fracture sites and shear bands where a significant temperature rise would be indicated by melted tin droplets.

Chapter 3

Results and Discussion

As previously stated, serrations or load drops found in stress-strain or stress-time curves in compression testing of metallic glasses indicate a period in the test when a shear banding event occurred to relieve the applied load. Figure 3.1 is part of an engineering stress versus time curve for one sample tested that did not fracture. The time on the bottom axes refers to a reference time just before the first serration occured. The thirteen serrations numerated in the figure occur primarily near the end of the elastic portion of the stress curve. In more ductile metallic glasses it is possible for over one hundred serrations to occur and extend far into the plastic portion of the curve. However, with the larger and much more brittle specimens used here, testing was arrested after only a few serrations were observed in the live load-time data to ensure they did not fracture.

The load data was acquired at 100 kHz, or one data point every 10 μs, making

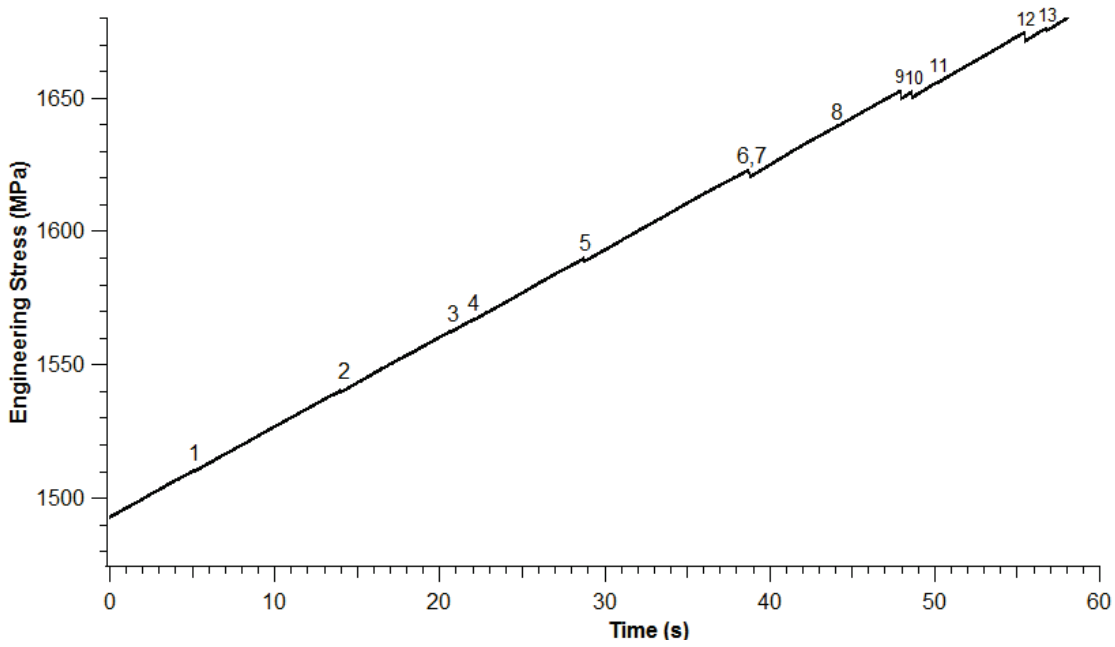

Figure 3.1: Engineering stress versus time data for one sample not brought to fracture. Indicated on the graph are the serrations representing a shear banding event in testing.

it possible to accurately measure the change in load and time where each of these serrations occur. Table 3.1 summarizes the load drop and time lapse of each shearing event seen in Fig. 3.1. Although it is not possible to associate a specific serration with a particular shear band on a specimen, it is noted that for the thirteen load drops identified in the data from this sample the durations of the shear events range from 2.32 ms to 6.52 ms with an average of 4.65 ms and the load drops ranged from 0.26 MPa to 3.02 MPa with an average of 1.17 MPa. It is clear from the measured time lapses that the duration of these shear banding events is orders of magnitude longer than previously assumed in many heat evolution calculations.

Serration #	Shear Time (ms)	Load Drop (MPa)
1	3.75	0.39
2	5.73	0.46
3	4.15	0.26
4	5.39	0.33
5	5.72	1.12
6	2.32	1.44
7	3.41	1.31
8	6.52	0.33
9	3.37	2.89
10	4.15	2.24
11	5.38	0.40
12	6.00	3.02
13	4.50	0.99
Averages	**4.65**	**1.17**

Table 3.1: Time lapse and load drop of each serration measured from data represented in Fig. 3.1.

To round out the analysis of the shear banding events, the data from Table 3.1 is plotted in Fig. 3.2. No trend was found in the data to connect shear event duration and load drop, which augments the assertion that shear banding is largely unpredictable.

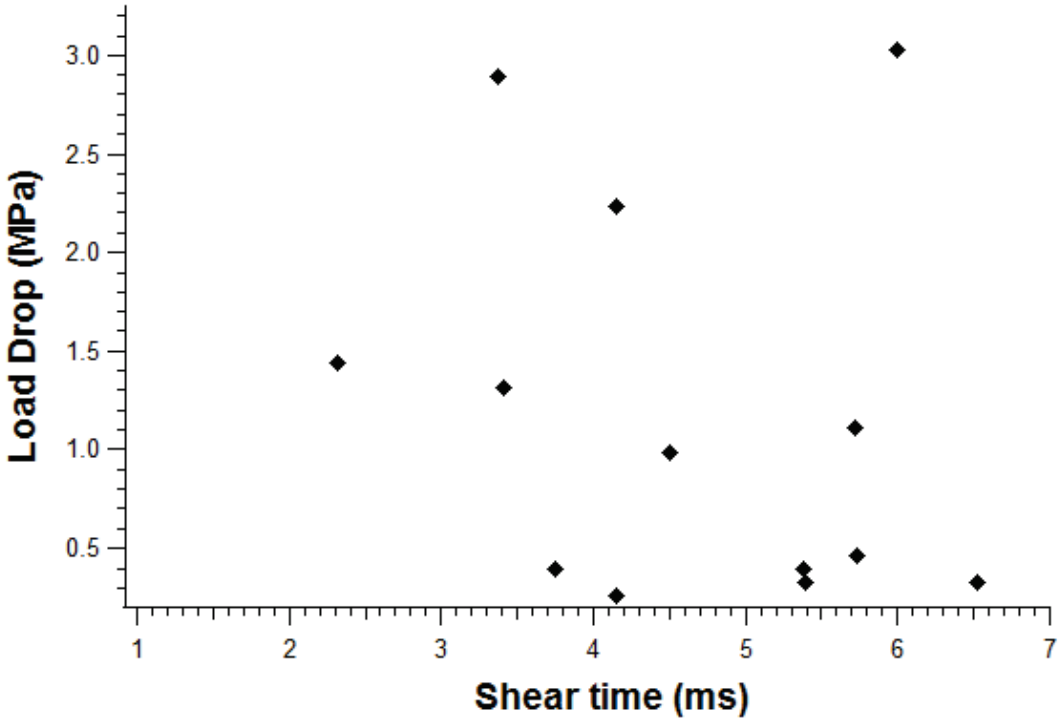

Figure 3.2: A plot representing data tabulated in Table 3.1 of load drops vs. shear times for each serration.

Now, to find the maximum temperature rise that could reasonably be calculated from this data the largest load drop should be considered. If it is assumed all the work done in shearing goes into heating the shear band, the strain energy can be taken as the change of area under the stress-strain curve due to the serration. Hence, the

largest load drop would result in the largest heat content. A close up of this specific serration with the largest load drop is shown in Fig 3.3.

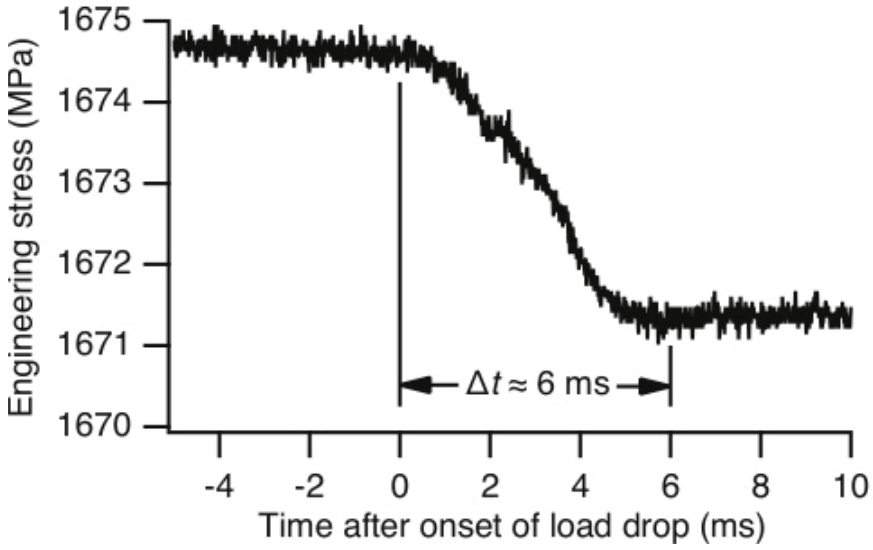

Figure 3.3: A close up of serration no. 12 in Fig. 3.1 and Table 3.1.

The change in elastic strain energy density (Δh) in shearing can be visualized using Fig. 3.4, where the change in area due to a serration is represented in the top dark-shaded triangle. From this graphic, Δh of a specimen that experiences a load drop of $\Delta\sigma$ at a flow stress σ can be calculated by Equation 3.1,

$$\Delta h \simeq \left(\frac{\sigma}{E}\right)\Delta\sigma \tag{3.1}$$

where E is Youngs Modulus. If we treat the shear band as a planar source of heat, the average thermal flux out of the shear band can then be taken as the strain energy multiplied by the shear velocity (Equation 3.2).

$$q \approx \Delta h \times \left(\frac{l}{t}\right) \tag{3.2}$$

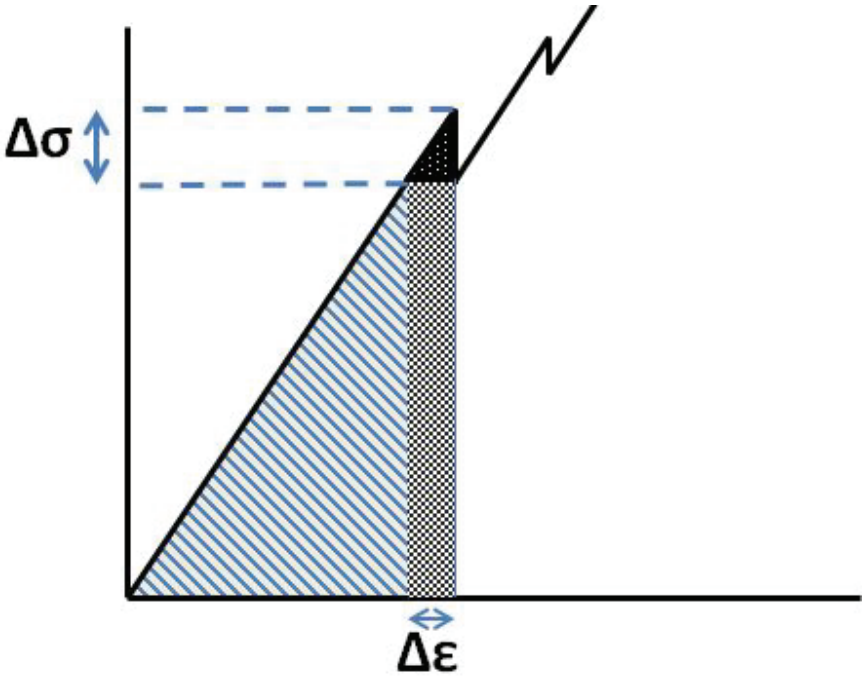

Figure 3.4: A sketch work done in shearing by changes of stress and strain in a serration.

The shear velocity is taken as the length of the shear band l over the shear time t based on high-speed cinematography that has shown that most of the slip occurs simultaneously across the entire shear band as opposed to a single propagating front [11].

Finally, the temperature rise $\Delta T(x,t)$ can be found using a one dimensional diffusion profile [20],

$$\Delta T(x,t) = \frac{q}{2c_p\alpha}\left(\sqrt{\frac{4\alpha t}{\pi}}\exp\left(\frac{-x^2}{4\alpha t}\right) - x\mathrm{erfc}\left(\frac{x}{\sqrt{4\alpha t}}\right)\right) \tag{3.3}$$

where c_p is the constant pressure heat capacity, α is the thermal diffusivity, t is the duration of shear event, and x is the distance from the shear band.

Parameter	Vitreloy 106 Value
Heat capacity, c_p	2.57×10^6 J/m^{3}K
Thermal diffusivity, α	3×10^{-6} m^2/s
Young's Modulus, E	96 GPa
Flow stress, σ_f	1850 MPa

Table 3.2: Material properties of the BMG Vitreloy 106.

To calculate temperature rise from this model we need values of load drops and shear times determined from the stress-time curve (Table 3.1) and certain constant material parameters. Because the specific metallic glass composition used here ($Zr_{57}Ti_5Cu_{20}Ni_8Al_{10}$) has not been extensively tested for each of these parameters, values for the common BMG Vitreloy 106 ($Zr_{57}Nb_5Cu_{15.4}Ni_{12.6}Al_{10}$) were used (Table 3.2) because of its similar composition.

While the specific temperature rise for each shear event in these experiments cannot be determined, it is possible to place bounds on the temperature rise. Using values from the largest load drop in the data shown in Fig. 3.3, the calculated maximum temperature increase at the center of the shear band (*i.e.* at x=0) as a function of shear time is shown in the bottom curve in Fig. 3.5. The maximum temperature rise is plotted in this fashion to highlight its dependence on duration of shearing event. Shown to the very right of the bottom curve is the experimental event with shear duration of $\sim$ 6 ms. Clearly with this time duration, or any duration on the order of milliseconds, the temperature rise is simply insignificant, calculated to

be only a fraction of a Kelvin.

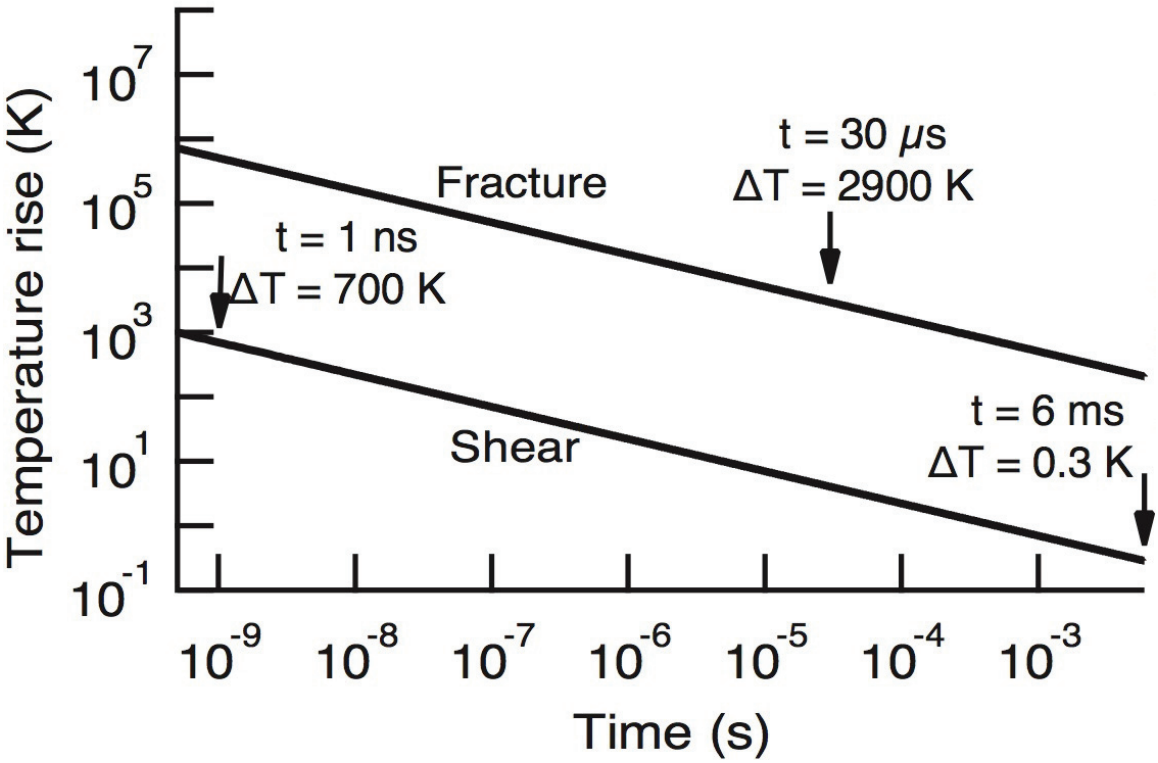

Figure 3.5: Calculations of maximum temperature rise versus time at the center of a shear band. The lower curve represents a shear band event with indicated times of our experimentally measured event (6 ms) and theoretical times often hypothesized (1 ns). The upper curve represents a fracture event with our experimentally measured fracture time (30 μs).

Closer SEM observation of the non-fractured samples corroborates these calculations of temperatures ries insufficient to melt the coating(Fig. 3.6). No melted tin was observed on any of the samples that did not fracture, even those with shear bands displaying significant shear offsets up to $\sim 6\mu$m.

Also indicated on the bottom curve is an assumed very fast shear time often inputted into temperature rise calculations ($\sim$ 1ns) [4, 17, 18]. It is noted that the calculations for very short shear durations predicts significant temperature rises, validating the analysis and assertion that heating is principally dependent on event duration.

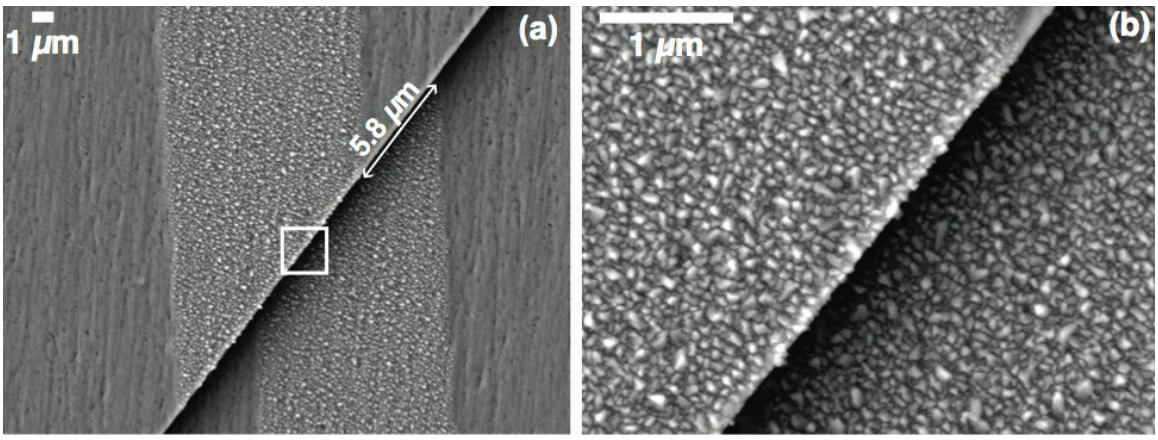

Figure 3.6: Scanning electron micrographs of tin lines after testing on a non-fractured spceimen. Shear bands displaying large shear offsets (a) showed no melted tin upon a closer look (b).

In order to verify the hypothesis further, the same analysis was performed on specimens that were brought to fracture. Figure 3.7 shows the stress-time curve for one of these samples. The fracture data shows the time for the event to occur is $\sim 30\mu$s. Because this load drop is extremely large compared to the small serrations seen in shear banding, there is simply a much larger amount of energy released in a much shorter time. Using the same thermal analysis with a new t and $\Delta\sigma$, the

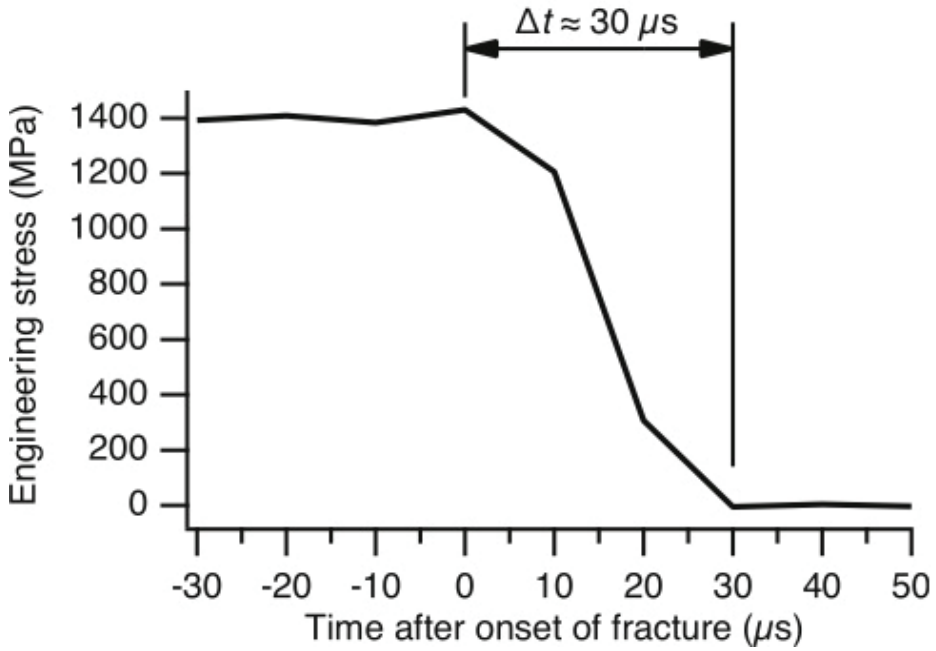

Figure 3.7: Stress versus time data of a fracture event.

maximum temperature rise for this fracture event was plotted in the top curve of Fig. 3.5. Indicated in the plot is the maximum temperature rise for the specific fracture time, 2900 K and 30 μs respectively. With a significant temperature increase predicted by the data, it is expected that the tin would melt on these samples. And indeed, on these fractyred specimens the temperature increase was sufficient to melt the tin coating, as evidenced in Fig. 3.8.

While the observations support this analysis, these calculations are only an estimate. As previously mentioned, one serration in load data cannot be matched with any specific shear band. However, if all calculated temperature increases from each serration were attributed to one shear banding event an extremely unlikely scenario

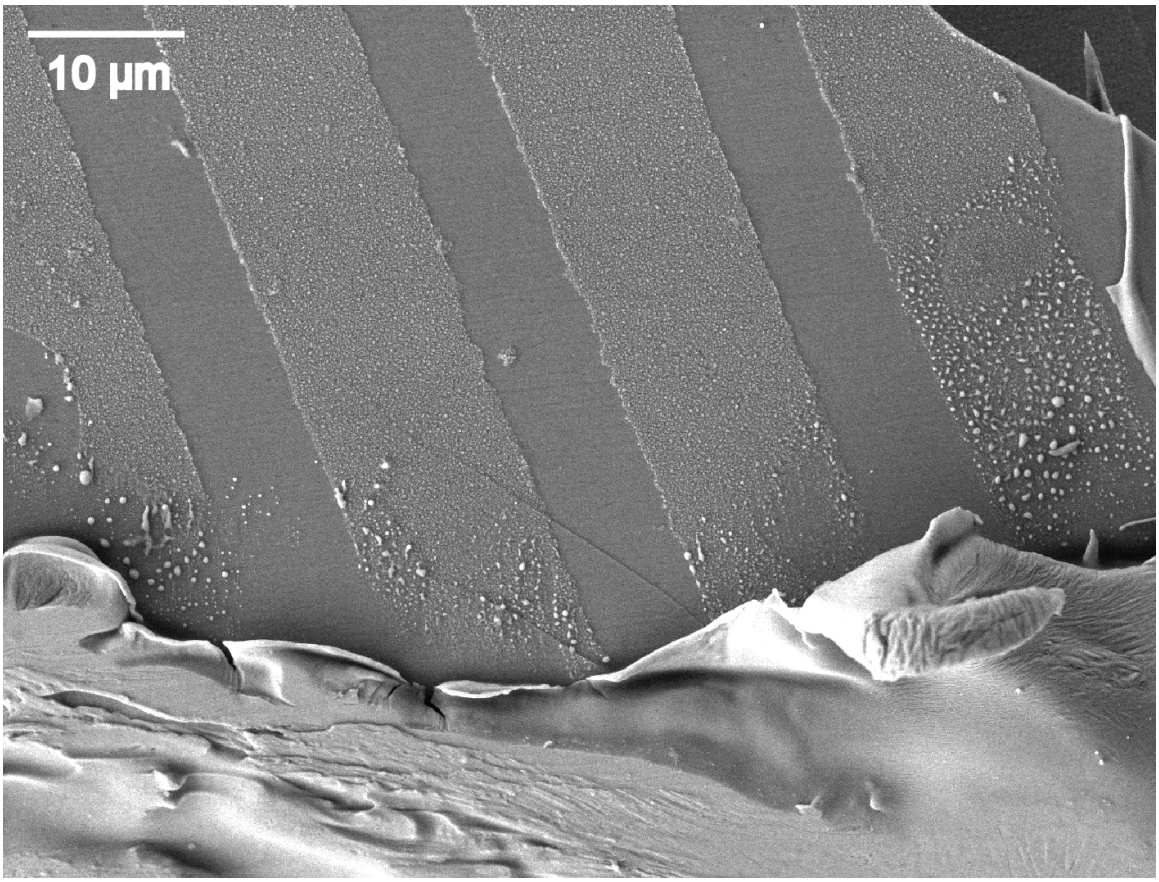

Figure 3.8: Scanning electron micrographs of tin lines near a fracture surface.

the sum would still be very insufficient to melt the tin coating. Also, it is noted that all of the elastic strain energy released in fracture may not go into heating the fracture surface. At the same time strain energy from the compression machine may contribute to melting of the fracture surface. Additionally, with the very few data points outlining the fracture event it is possible the event is over before the first stress value of "0" is read. Nevertheless, it is the orders of magnitude of the calculated temperature increases which are most important. Aside from large unknown influences

in testing, any reasonable fluctuations in the data and calculations still results in the same conclusions.

Chapter 4

Conclusion

The results and obersvations in this work are comparable with several other reports agreeing with the conclusion that there is no significant heating during the normal deformation of bulk metallic glasses. The implications of this conclusion are important because shear band heating and velocity are fundamentally linked to the underyling deformation mechanisms. Our calculations propose that the temperature increase in shear bands is not significant enough to be the driving force for their generation or propagation. Furthermore the differences in time measured from the shear banding events and fracture events suggests that fracture is not simply the extension of a shear band to failure. Although the connection between the inital deformation and final failure of metallic glasses is still largely unknown, resolutions of experimental methods are steadily improving to shed light on these events. In order for bulk metallic glasses to realize their full potential in structural and other components, these fundamental

questions must be answered by advanced computer simulations heavily supplemented by innovative experiments such as this and those which lead to the development of this project.

Vita

Stephanie Slaughter is a Master's student at Johns Hopkins University pursuing her M.S. in Materials Science and Engineering. As a member of Dr. Hufnagel's research group she has focused her research on deformation of bulk metallic glasses. She aslo performs research at the Army Research Lab in Aberdeen, MD working on integrating a femtosecond laser into an SEM for machining and serial sectioning purposes. Starting Fall 2014 she will be attending the University of Pennsylvania to obtain her Ph.D., also Materials Science and Engineering with a focus on nanotechnology.